Neuron
Report

Optimization of Somatic Inhibition at Critical Period Onset in Mouse Visual Cortex

Hiroyuki Katagiri,[1,3] Michela Fagiolini,[1,4] and Takao K. Hensch[1,2,4,5,*]
[1] Laboratory for Neuronal Circuit Development, RIKEN Brain Science Institute, 2-1 Hirosawa, Wako-shi, Saitama 351-0198, Japan
[2] Core Research for Evolutional Science and Technology, Japan Science and Technology Agency, Osaka 560-0082, Japan
[3] Present address: Lab for Perception and Memory, Institut Pasteur, 25 Rue du Dr. Roux, 75724 Paris, Cedex 15, France.
[4] Present address: Division of Neuroscience, Children's Hospital Boston, Harvard Medical School, 300 Longwood Avenue, Boston, MA 02115, USA.
[5] Present address: Department of Molecular and Cellular Biology, Center for Brain Science, Harvard University, 7 Divinity Avenue, Cambridge, MA 02138, USA.
*Correspondence: hensch@mcb.harvard.edu
DOI 10.1016/j.neuron.2007.02.026

SUMMARY

Local GABAergic circuits trigger visual cortical plasticity in early postnatal life. How these diverse connections contribute to critical period onset was investigated by nonstationary fluctuation analysis following laser photo-uncaging of GABA onto discrete sites upon individual pyramidal cells in slices of mouse visual cortex. The $GABA_A$ receptor number decreased on the soma-proximal dendrite (SPD), but not at the axon initial segment, with age and sensory deprivation. Benzodiazepine sensitivity was also higher on the immature SPD. Too many or too few SPD receptors in immature or dark-reared mice, respectively, were adjusted to critical period levels by benzodiazepine treatment in vivo, which engages ocular dominance plasticity in these animal models. Combining GAD65 deletion with dark rearing from birth confirmed that an intermediate number of SPD receptors enable plasticity. Site-specific optimization of perisomatic GABA response may thus trigger experience-dependent development in visual cortex.

INTRODUCTION

Inhibition in the brain is mediated by a rich diversity of GABAergic interneurons (Markram et al., 2004). These local circuits target specific subdomains on nearby pyramidal cells, such as the soma-proximal dendrite (SPD) region or axon initial segment (AIS). This distribution of labor suggests highly precise points of information transfer and regulation (Nicoll, 1994; Pouille and Scanziani, 2004). In the developing visual cortex, specific $GABA_A$ circuits incorporating the α1 subunit mediate the competition between eyes, known as ocular dominance plasticity (Fagiolini et al., 2004). Interestingly, these subunits are enriched opposite parvalbumin (PV)-positive synaptic boutons innervating the SPD but not the AIS (Klausberger et al., 2002).

We, therefore, examined these two sites at high spatial resolution to determine whether the SPD selectively exhibits maturational changes predictive of critical period (CP) onset. Sensitivity to monocular occlusion appears around the fourth postnatal week (>P22) in parallel with the development of inhibitory responses (Komatsu and Iwakiri, 1991). Dark rearing from birth delays both the onset of the CP (Mower, 1991; Fagiolini et al., 1994; Hensch and Fagiolini, 2005) and the functional maturation of inhibition onto pyramidal cells (Benevento et al., 1992; Morales et al., 2002). However, macroscopic assays (spiking, miniature IPSCs) do not identify which of the many subtypes of inhibitory circuit are changing.

Both pre- and postsynaptic changes could potentially contribute to altered inhibitory transmission. It remains controversial whether postnatal development of GABA immunoreactive cells or receptors occurs normally in the absence of visual input (Benevento et al., 1995; Mower et al., 1988). Iontophoresis of GABA in dark-reared (DR) kittens has in fact suggested that development or maintenance of GABA receptors is not critically dependent on visual experience (Tanaka et al., 1987). Here, we circumvented the presynaptic component and directly assayed GABA response by laser photo-uncaging of neurotransmitter onto the SPD and AIS sites of individual pyramidal cells in slices of mouse visual cortex. In addition to examining development from pre-CP into CP, we examined DR mice and benzodiazepine (BDZ) sensitivity in animals lacking a synaptic isoform of glutamic acid decarboxylase (GAD65). The GAD65 knockout (KO) mouse fails to enter the CP due to poor GABA release from all inhibitory terminals, but can be made plastic by increasing GABA response with diazepam (DZ) (Hensch et al., 1998; Iwai et al., 2003). Natural CP timing can similarly be accelerated in immature wild-type mice (Fagiolini and Hensch, 2000; Fagiolini et al., 2004).

Our results reveal a dynamic regulation of $GABA_A$ receptor ($GABA_AR$) number specifically at the SPD that is

predictive of CP onset. Strikingly, neither too many nor too few SPD receptors are permissive of plasticity. Optimization of somatic inhibition offers a deeper understanding of, and potential therapeutic target for, amblyopia, a permanent behavioral consequence of reduced ocular dominance found in animals from mouse to man (Daw, 1995; Prusky and Douglas, 2003).

RESULTS

$GABA_A$ Response at the SPD and AIS Sites

To investigate the functional role of GABAergic inhibition at discrete sites upon single pyramidal cells, we employed laser photo-uncaging of neurotransmitter (Katz and Dalva, 1994; Pettit and Augustine, 2000). First, we characterized the focal spot size by immunocytochemical and electrophysiological methods. A living brain slice was incubated in solution containing anti-$GABA_AR$ α1 subunit antibody, as well as secondary anti-rabbit IgG and caged fluorescein conjugate, then transferred to a laser photo-uncaging recording chamber. After passive diffusion of biocytin from the whole-cell recording pipette into a layer 2/3 pyramidal cell in binocular visual cortex (Figure 1A), an ultraviolet (UV) laser was flashed at one site on the cell soma, and green epifluorescence revealed a spot diameter of about 4 μm (Figures 1B and 1C).

Whole-cell voltage-clamp recording was performed in unstained slices superfused with perfusate containing caged GABA (20 μM). Illumination of the SPD site by a brief UV pulse elicited the largest response to uncaged GABA (Figure 1D), while little or no response was observed at sites more than 25 μm away from the soma. Thus, our laser photo-uncaging system was adequate for mapping focal GABA responses at multiple, discrete sites within a highly restricted radius upon single cells.

In the following experiments, we then compared responses to 10 μM uncaged GABA at the SPD and AIS site, where little $GABA_AR$ α1 subunit is found (Nusser et al., 1996; Fritschy et al., 1998; Klausberger et al., 2002). After visually and physiologically determining the SPD site, we aligned the AIS site, separated across the cell soma by 25 μm opposite the apical dendrite. The average reversal potentials for GABA responses at SPD and AIS sites were -62.6 ± 0.8 and -62.6 ± 1.5 mV, respectively (Figure 1E), close to the predicted chloride reversal potential of -64 mV. In addition, the $GABA_AR$ antagonist bicuculline completely abolished these outward currents at a holding potential of -30 mV (Figure 1F). These results confirmed that responses to photoreleased GABA at both sites were mediated by $GABA_AR$.

Global inhibition within visual cortex is reported to be regulated by both age and visual experience (Benevento et al., 1992; Chen et al. 2001; Heinen et al., 2004; Komatsu and Iwakiri, 1991; Morales et al., 2002). We first examined the developmental profile of individual responses to photoreleased GABA at both sites as animals matured after eye-opening. The baseline amplitude of GABA response

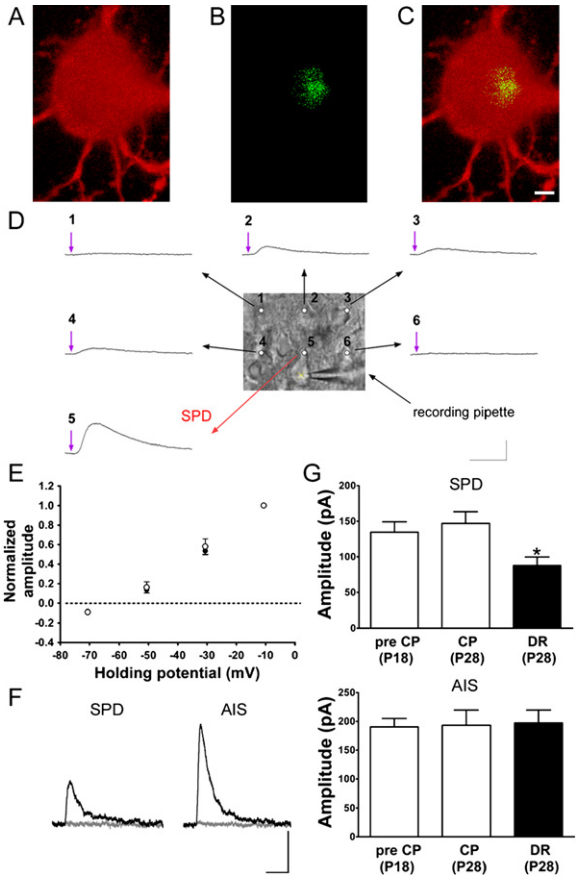

Figure 1. Laser Photo-Uncaging at SPD and AIS Sites

(A) Biocytin-injected layer 2/3 pyramidal cell in primary visual cortex (red). (B) Focal uncaging of fluorescein-conjugated secondary antibody (green) reveals UV laser spot size. (C) Merged image of (A) and (B). Scale bar, 4 μm. (D) Functional spatial resolution of laser photo-uncaging (white circles). UV flash (purple arrow) at SPD site (spot #5) produced a large response to uncaged GABA, while little or no response was observed 25 μm away in any direction. Some spots may be located on dendrites of the recorded pyramidal cell (spots #2, #3, and #4). Scale bars, 250 pA, 50 ms. (E) Current-voltage relationship of peak GABA response amplitude at SPD (white circle) and AIS (black circle) sites reveals identical slope and reversal potential. Amplitudes were normalized to the value obtained at -10 mV membrane potential. Plots represent mean ± SEM (three slices). (F) Blockade of GABA responses at both sites by a $GABA_AR$ antagonist, bicuculline (10 μM, gray traces). Scale bars, 100 pA, 100 ms. (G) Comparison of GABA responses to uncaged GABA at both sites in pre-CP (SPD: 9 slices, 8 mice; AIS: 11 slices, 9 mice), CP (SPD: 9 slices, 7 mice; AIS: 9 slices, 9 mice) and DR (SPD: 11 slices, 9 mice; AIS: 11 slices, 9 mice).

at both sites remained unaltered from pre-CP into CP ages ([SPD] pre-CP: 134.6 ± 14.5 pA; CP: 146.9 ± 16.6 pA; $p > 0.05$; [AIS] pre-CP: 190.3 ± 14.6 pA; CP: 193.3 ± 26.4 pA; $p > 0.05$) (Figure 1G).

Dynamic Regulation of Somatic $GABA_AR$

We next used DR mice to assess the effect of visual experience on $GABA_AR$-mediated currents. Animals reared in complete darkness from birth to the fourth postnatal

week exhibit a delayed onset of the typical CP (Mower, 1991; Hensch and Fagiolini, 2005). Surprisingly, dark rearing selectively reduced the magnitude of GABA response amplitude only at the SPD site, with no effect on the AIS response ([SPD] DR: 87.7 ± 12.1 pA; CP versus DR, $p < 0.05$; [AIS] DR: 197.2 ± 22.5 pA; CP versus DR, $p > 0.05$) (Figure 1G).

We therefore turned to a detailed analysis of GABA plasticity at the SPD site. To estimate single-channel conductance and the number of open $GABA_AR$ channels at each site, we performed nonstationary fluctuation analysis (Traynelis et al., 1993). This revealed the number of open channels at the SPD site to be significantly decreased in DR mice (CP: 126.1 ± 11.9; DR: 60.0 ± 11.2; $p < 0.05$), while single-channel conductance was no different from light-reared mice of the same age (CP: 47.9 ± 8.4 pS; DR: 49.8 ± 5.8 pS; $p > 0.05$) (Figure 2C). In contrast, at the AIS site no clear change in single-channel conductance (CP: 34.3 ± 4.6 pS; DR: 24.9 ± 2.5 pS; $p > 0.05$) or number of open channels (CP: 222.1 ± 31.3; DR: 323.4 ± 48.9; $p > 0.05$) was found after dark rearing, consistent with unaltered amplitude measurements (Figure 1G, bottom).

We then revisited the developmental profile of GABA response at the SPD site. No change in overall amplitude (Figure 1G) could mask a concomitant regulation of receptor conductance and number in opposite directions. Indeed, as light-reared animals normally matured into the CP, single-channel conductance at the SPD site was significantly increased (pre-CP: 24.44 ± 2.7 pS; versus CP, $p < 0.05$), while the number of open channels was significantly decreased (pre-CP: 195.2 ± 24.2; versus CP, $p < 0.05$) (Figure 2C). Instead, at the AIS site neither receptor number (pre-CP: 288.0 ± 26.8) nor conductance (pre-CP: 29.4 ± 3.4 pS) was altered with age (pre-CP versus CP, $p > 0.05$) (Figure 2D). Taken together, these results reveal a highly dynamic, subcellular regulation of $GABA_AR$ by age and sensory experience at discrete sites within single neurons. CP onset in particular may reflect the enhanced function of a reduced $GABA_AR$ number at the SPD site.

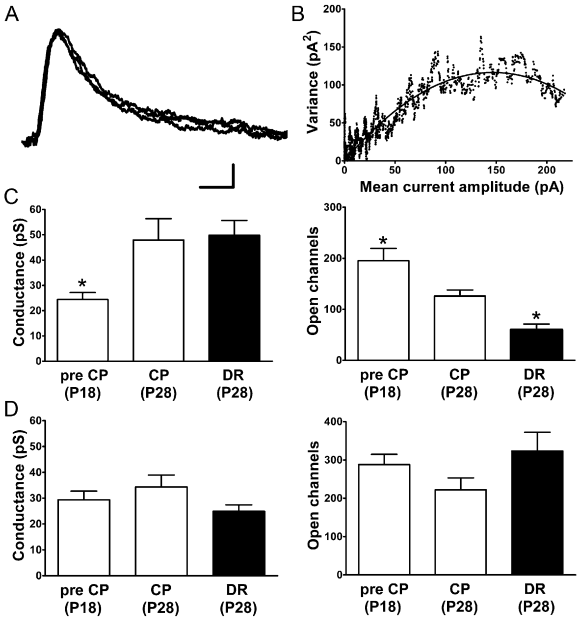

Figure 2. Selective and Dynamic Regulation of GABA Response at the SPD Site by Age and Experience

(A) Representative, superimposed consecutive traces. Scale bars, 50 pA, 25 ms. (B) Fluctuation analysis of the same neuron. Variance of the decay phase about the mean for individual GABA responses is plotted as a function of the mean current after the peak. Solid line shows parabolic fit of the relationship. (C and D) Estimated single-channel conductance (left) and number of open channels (right) for GABA responses at the SPD (C) and AIS (D) sites. Both the number of open channels and single channel conductance change only at the SPD site with CP onset (pre-CP versus CP, *$p < 0.05$). Dark rearing reduced the number of open channels only at the SPD site (CP versus DR, *$p < 0.05$). Data are from cells in Figure 1G.

DZ Favors Immature Somatic $GABA_A$ Response

We have previously shown that a functional enhancement of inhibition with BDZ agonists can trigger the CP in visual cortex of pre-CP wild-type and GAD65 KO mice (Hensch, 2005). To examine which site on individual pyramidal cells is affected by acute drug injection, we directly compared BDZ sensitivity at both the SPD and AIS in vitro. Bath application of DZ produced an increase in the magnitude of GABA response amplitude at both sites (Figure 3). However, this potentiation was significantly greater for the SPD than the AIS of single cells in pre-CP mice (SPD: 1.47 ± 0.23; AIS: 1.14 ± 0.05; $p < 0.05$). This relative difference disappeared as animals matured into the CP (SPD: 1.62 ± 0.24; AIS: 1.55 ± 0.25; $p > 0.05$) (Figures 3C and 3F). Similar to pre-CP wild-type animals, even in older GAD65 KO mice, application of DZ enhanced GABA responses at the SPD significantly more strongly than responses at the AIS (SPD: 1.64 ± 0.37; AIS: 1.36 ± 0.29; $p < 0.05$) (Figure 3I). These results suggest that when DZ is injected in an immature visual cortex (Hensch et al., 1998; Fagiolini and Hensch, 2000; Fagiolini et al., 2004), it preferentially enhances the GABA response at the SPD site to trigger the CP.

We then examined the number of somatic $GABA_AR$ following repeated BDZ injections. Four-day treatment with Zolpidem (Zol), which exhibits specificity for α1-containing receptors (Sanna et al., 2002), significantly decreased the number of SPD receptors in pre-CP mice (chronically Zol-treated: 113.5 ± 19.6; versus pre-CP, $p < 0.05$) to the same level as that of CP wild-type mice ($p > 0.05$) (Figure 4A). Similarly, chronic DZ treatment significantly reduced the number of open channels at the SPD site in GAD65 KO mice (control KO: 250.8 ± 44.9; versus chronically DZ-treated KO: 113.8 ± 18.6; $p < 0.05$) (Figure 4B). In addition, we found that DZ treatment in DR mice prevented somatic $GABA_AR$ from decreasing (chronically DZ-treated DR: 132.4 ± 27.2; versus control DR, $p < 0.05$), maintaining SPD receptor number at a CP level ($p > 0.05$) (Figure 4A). Notably, such DZ injection triggers the CP for ocular dominance even in complete darkness (Iwai et al., 2003).

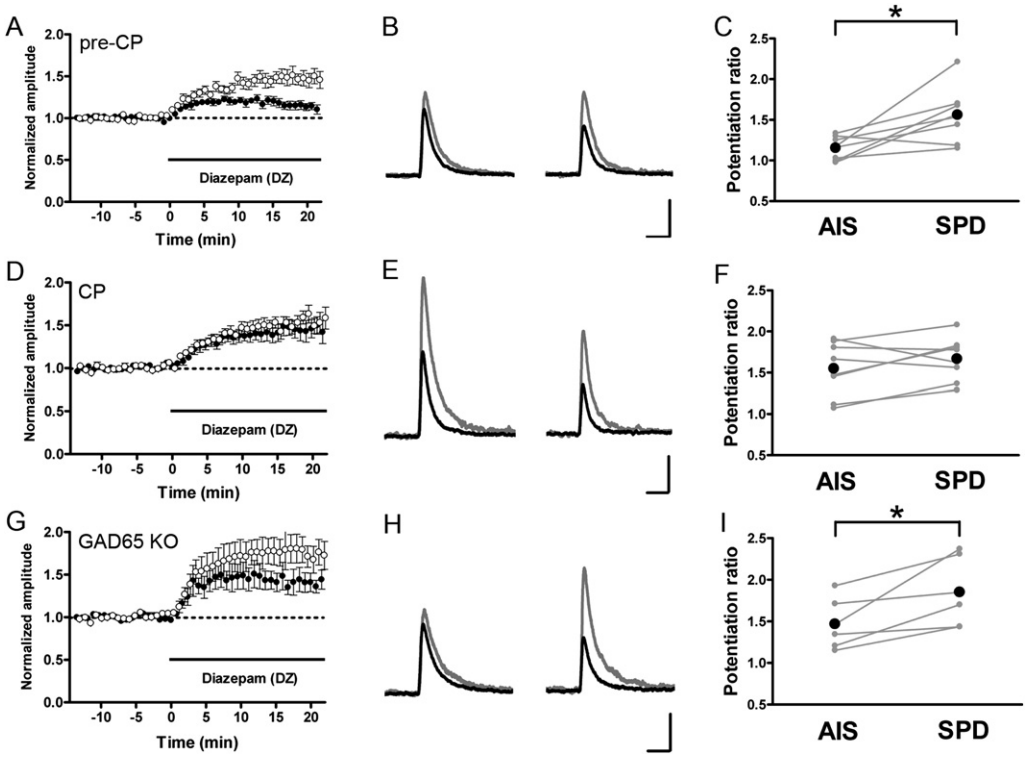

Figure 3. Higher Benzodiazepine Sensitivity at the SPD than at the AIS before the CP

(A, D, and G) Bath application of DZ (black bar) enhanced $GABA_A$R-mediated responses at both SPD (white circle) and AIS (black circle) sites in pre-CP (A, eight slices: seven mice), CP (D, eight slices: seven mice), and GAD65 KO (G, six slices: five mice) mice. Amplitudes normalized to baseline mean. Plots represent mean ± SEM. (B, E, and H) Representative GABA responses before (black) and during (gray) DZ treatment at both AIS (left) and SPD (right) sites (B, pre-CP; E, CP; and H, GAD65 KO mice). Scale bars, 100 pA, 100 ms. (C, F, and I) Preferential DZ sensitivity of SPD on individual pyramidal cells (gray circle) in pre-CP (C) and GAD65 KO mice (I) compared with CP (F) (pre-CP, GAD65 KO, *$p < 0.05$). Black circle indicates mean. Potentiation ratio was calculated once drug response stabilized (mean at 18–22 min).

Plasticity Rescued by Dark Rearing GAD65 KO Mice

We noted that the number of $GABA_A$R at the SPD site is regulated in similar directions by DZ treatment of GAD65 KO mice and dark rearing of wild-type mice. Since ocular dominance shifts by monocular deprivation are restored by DZ (Hensch et al., 1998), we wondered how the number of $GABA_A$R on the soma might change when GAD65 KO mice are reared in total darkness. Dark rearing also reduced the number of open channels at the SPD site of GAD65 KO mice to be comparable with the value in chronic DZ-treated animals (DR KO: 126.5 ± 12.0; versus control KO, $p < 0.05$; versus chronically DZ-treated, $p > 0.05$) (Figure 4B). This raised the possibility that dark rearing alone might rescue the ocular dominance plasticity of GAD65 KO mice, if the optimal inhibition for CP onset is determined by the number of $GABA_A$R underlying somatic inhibition.

To explore this idea directly, extracellular single-unit recordings were performed after a 4 day period of monocular occlusion in GAD65 KO mice dark reared until the fourth postnatal week. Monocular deprivation produced a robust ocular dominance shift toward the open, ipsilateral eye in DR GAD65 KO mice (Figure 4C) ($p < 0.0001$). The number of $GABA_A$R at the SPD site thus accurately predicts onset of the CP for ocular dominance plasticity.

DISCUSSION

Our findings indicate that a decrease in somatic $GABA_A$R number signals the natural onset of a physiological CP for visual cortical development. The subcellular specificity of this regulation reinforces previous evidence identifying $\alpha 1$ subunit containing $GABA_A$R (enriched at somatic PV-cell contacts) as a CP trigger (Fagiolini et al., 2004). Strikingly, an optimized inhibition appears crucial, as neither too many (pre-CP, GAD65 KO) nor too few (DR wild-type) receptors support ocular dominance plasticity (Figure 4A; Hensch, 2005). This principle was revealed by focal, photo-uncaging of neurotransmitter, which samples both synaptic and extrasynaptic $GABA_A$R, suggesting a dynamic model of receptor regulation by age and experience (Figure 4D).

In pre-CP mice, there may be many extrasynaptic $GABA_A$R on the soma that are activated by spillover of GABA released from ingrowing PV axon terminals. As these inputs strengthen and enwrap their perisomatic

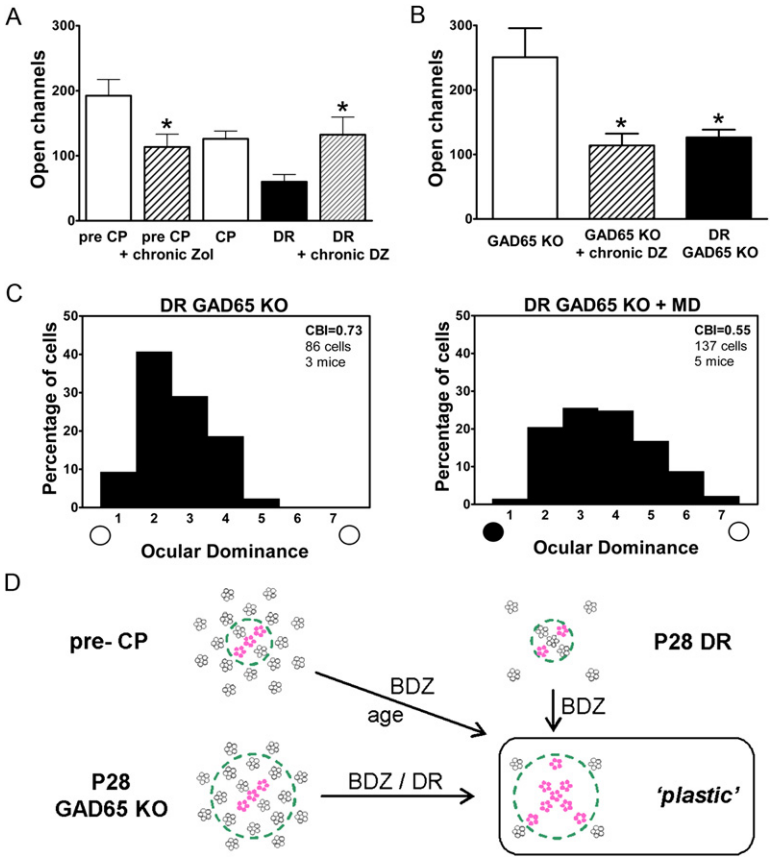

Figure 4. Optimal Number of Somatic $GABA_AR$ Underlying Ocular Dominance Plasticity

(A) Estimated number of open channels for GABA response at the wild-type SPD site in pre-CP Zolpidem-treated (five slices: three mice), typical CP (from Figure 2C), and DR + DZ-treated (six slices: five mice) mice is in an intermediate range that is permissive of plasticity in vivo (pre-CP versus pre-CP + Zolpidem, DR versus DR + DZ; *$p < 0.05$).

(B) Estimated number of open channels for GABA response at SPD site in control (nine slices: nine mice), DZ-treated (five slices: four mice), and DR (ten slices: nine mice) GAD65 KO mice. Both DZ injection and DR similarly rescue $GABA_AR$ number (KO versus KO + DZ, KO versus DR KO; *$p < 0.05$).

(C) Ocular dominance distribution of GAD65 KO mice reared in total darkness is normally skewed in favor of the contralateral eye (left). Subsequently, a shift toward the open, ipsilateral eye by 4 days of monocular eyelid suture is rescued in these mice (right), similar to the consequences of DZ treatment (Hensch et al., 1998).

(D) Ocular dominance plasticity is enabled by optimal somatic inhibition, when the number of saturated $GABA_AR$ (pink) may best match the overlying terminal bouton function of PV-positive axons (dashed green ring).

target, unsaturated $GABA_AR$ disappear and saturated $GABA_AR$ become concentrated underneath the synaptic terminal, a process that perhaps involves receptor diffusion in the membrane (Bogdanov et al., 2006). Initially small receptor clusters may be recruited into larger clusters of high conductance with the maturation of GABAergic innervation (Christie et al., 2002; Hutcheon et al., 2004). Accordingly, we found that single-channel conductance of $GABA_AR$ at the SPD increases with age (Figure 2C; Fritschy et al., 1994; Heinen et al., 2004).

In an immature visual cortex (pre-CP, GAD65 KO, DR wild-type), positive modulators like DZ may trigger CP onset through the regulation of $GABA_AR$ number. The balance between endocytosis and exocytosis reflects the total amount of $GABA_AR$ on the cell surface (Choquet and Triller, 2003). Less functional extrasynaptic receptors may be routinely lost (Akaaboune et al., 1999), while BDZs help to promote receptor maintenance by fully saturating GABA response beneath the nascent synapse, especially when transmitter release is weak (pre-CP, GAD65 KO). With age, presynaptic structure, function, and GABA content would normally increase to play this role.

Since extrasynaptic receptors control the amount of somatic $GABA_AR$ (Choquet and Triller, 2003), it is important to consider how tonic GABA release regulates the CP even in the complete absence of vision (Iwai et al., 2003). In DR mice, both excitation and inhibition are reduced, leading to an exaggerated age-dependent removal of $GABA_AR$ (Figures 4A and 4D). Homeostatic mechanisms detect net circuit activity and adjust inhibition downward when excitation is weak (Kilman et al., 2002; Turrigiano and Nelson, 2004). Genetically weakened GABA release in the absence of GAD65 may itself offset reduced excitation in the dark and attenuate this homeostatic component. Hence, $GABA_AR$ number is less downregulated by dark rearing in these mutant mice (Figures 4B and 4D).

Consistently, ocular dominance plasticity is possible when SPD receptor number is in the intermediate range (~100 channels) between immature pre-CP/GAD65 KO (~200 channels) and DR wild-type (~50 channels) levels. We predict this optimization reflects a matching of postsynaptic receptor function to presynaptic terminal size (dashed green circles, Figure 4D). Indeed, the number of immunogold-labeled $GABA_AR$ particles at mature synapses is linearly proportional to junctional area (Nusser et al. 1997). Since GAD67 plays a predominant role in PV axon terminal maturation (Soghomonian and Martin, 1998; Chattopadhyaya et al., 2006), perisomatic bouton formation in the absence of the alternate isoform GAD65 is expected to be normal in size. Without sensory input through the third postnatal week, perisomatic boutons

fail to proliferate or extend terminal branches in DR mice (Chattopadhyaya et al., 2004). The GABA transporter (GAT1) is ideally situated to coordinate the balance of synaptic versus extrasynaptic $GABA_AR$ activation (Cherubini and Conti, 2001). Postsynaptic receptor activation could then retrogradely signal presynaptic arbor maturation (Sanes and Lichtman, 2001). An intriguing molecular mechanism may involve BDNF, which can induce both a reduction in $GABA_AR$ number and presynaptic change (Henneberger et al. 2005).

Alteration of $GABA_AR$ function poses important consequences for proper neuronal excitation. Once optimized, a site-specific regulation of synaptic efficacy based on $GABA_AR$ number between fast-spiking PV-cells and neighboring pyramidal cells may maintain the effects of monocular occlusion (Maffei et al., 2006). Disorders of local circuit activity derive in part from a modification of postsynaptic $GABA_AR$ expression (Kittler and Moss, 2003; Fritschy and Brünig, 2003). In the kindling model of temporal lobe seizures, $GABA_AR$ at synapses on the soma and AIS of dentate gyrus granule cells increases in number (Nusser et al., 1998). Apart from amblyopia and epilepsy, several other neurological and psychiatric disorders are now thought to result from abnormal excitatory-inhibitory balance in key systems (Fritschy and Brünig, 2003). Our findings may thus be of broad relevance to the understanding of anxiety disorders (Nutt and Malizia, 2001), ethanol dependence (Morrow et al., 2001), Huntington's disease (Kunig et al., 2000), Angelman syndrome (DeLorey et al., 1998), Rett Syndrome (Dani et al., 2005), autism (Rubenstein and Merzenich, 2003), or schizophrenia (Lewis et al., 2005). Optimization processes for $GABA_AR$ signaling may be fruitful targets for novel therapeutic approaches.

EXPERIMENTAL PROCEDURES

For most experiments, wild-type (C57Bl/6, pre-CP: 18–20 days old, CP: 27–32 days old) or GAD65 KO (27–31 days old) mice were reared with normal visual experience (12 hr light/dark cycle). Chronically BDZ-treated mice were prepared by 4 day DZ (2 mg/ml; Wako Pure Chemical, Osaka, Japan) or Zol (100 μM, Tocris) injection into both lateral ventricles (1.5 μl/hemisphere). In some experiments, mice were kept in a dark-room from birth to P27–32 days. Coronal slices (350 μm) were prepared from the binocular zone of mouse visual cortex after halothane anesthesia, decapitation, and brain removal. After cutting, slices were incubated in oxygenated artificial cerebrospinal fluid (ACSF) for at least 1 hr (room temperature). The ACSF contained 119 mM NaCl, 2.5mM KCl, 1.3 mM $MgCl_2$, 10 mM NaH_2PO_4, 26.2 mM $NaHCO_3$, 2.5 mM $CaCl_2$, and 11 mM glucose. To confirm that only a limited area is photostimulated, one slice was first incubated in ACSF containing rabbit anti-GABA α1 subunit (60 min, Alomone), washed, then incubated in ACSF containing goat anti-rabbit IgG caged fluorescein conjugate (90 min, Molecular Probes) prior to photo-uncaging.

Each slice was perfused with ACSF (~3–4 ml/min) containing 10 μM γ-aminobutyric acid, γ-carboxy- 2-nitrobenzyl ester, trifluoroacetic acid salt (O-(CNB-caged) GABA), 10 μM 2, 3-Dioxo- 6-nitro-1,2,3,4-tetrahaydrobenzo [f]quinoxaline-7-sulfonamide disodium salt (NBQX), and 25 μM D-2-amino-5-phosphonovaleric acid (D-APV). Patch electrodes (3–6 MΩ) were filled with an internal solution (126 mM Cs gluconate, 8 mM CsCl, 20 mM HEPES, 0.2 mM EGTA, 2 mM NaCl, 3 mM Mg-ATP, 0.5 mM Na_3-GTP, and 0.15% biocytin) (pH 7.2, 290–300 mOsm). Whole-cell voltage-clamp recording from visualized layer 2/3 pyramidal cells was performed using infrared-Nomarski DIC optics (Olympus BX-50; Hamamatsu) and Axo-patch 1D amplifiers (Axon Instr.). Liquid junction potentials (~10 mV) were compensated.

After the SPD was identified by observation through a water-immersion lens (40×), the AIS was aligned and separated by 25 μm opposite the apical dendrite. UV light (8 ms flash from an argon-ion laser) was focused from above onto a 2 μm spot in the plane of the brain slice through a 40× microscope objective. Responses to uncaged GABA were recorded with 2 mW laser power at the front of the objective. The AIS, one distal site (>100 μm away from both AIS and SPD), the SPD, and another distal site were photostimulated sequentially every 10 s by computer-controlled, x-y movement of the objective. Series resistance (<20 MΩ) was monitored for stability throughout the recordings, and if changing >20%, the data were discarded. Records were filtered at 1 kHz (Brownlee Instr.), digitized at 13 kHz, and stored and analyzed using Experimenter's WorkBench (DataWave Technologies). All experiments were performed at 34°C.

Tissue slices containing biocytin-filled cells were fixed in 4% paraformaldehyde (4°C overnight). Slices were then washed three times in 0.1 M phosphate buffer (PB, pH 7.4) without resectioning, incubated with phosphate-buffered saline (PBS) containing Alexa 546 conjugated Streptavidin (Molecular Probes) and 0.25% Triton-X (2 hr, room temperature). After washing three times in PB, slices were observed under a confocal microscope (Leica).

In the fluctuation analysis, a series of 15 responses with stable amplitude and duration like the baseline period in Figure 3 were averaged. Plots of mean variance σ^2 against mean current I after the peak were well fit by a parabolic function as follows: $\sigma^2 - \sigma_{basal}{}^2 = iI - I^2/N$, where i is the current carried by a single open channel and N is the number of open channels. From i, the single channel conductance was calculated. Results were reported as mean ± SEM. In Figure 1G, Figures 2C and 2D, and Figures 4A and 4B, statistical significance was evaluated by Dunnett's multiple comparison test. Paired t test and χ^2 test were used to evaluate the data in Figures 3C, 3F, and 3I, and Figure 4C, respectively.

Single-unit recording was performed under Nembutal (50 mg/kg; Abbot)/chlorprothixene (0.2 mg; Sigma) anesthesia using standard techniques (Hensch et al., 1998). For each mouse, 25–30 single units in multiple penetrations were recorded (>200 μm intervals) across the medio-lateral extent of primary visual cortex to map the monocular and binocular zones and avoid sampling bias. Cells were assigned ocular dominance scores using a seven-point classification scheme. For each binocular zone, we calculated a contralateral bias index (CBI): $[(n_1 - n_7) + (2/3)(n_2 - n_6) + (1/3)(n_3 - n_5) + N]/2N$, where N = total number of cells, and n_x = number of cells with an ocular dominance score x. This weighted average of the bias toward one eye or the other takes values from 0 to 1 for complete ipsilateral or contralateral eye dominance, respectively. In monocular deprivation experiments, eyelid margins were trimmed and sutured under halothane anesthesia. All experiments were obtained contralateral to the deprived eye.

ACKNOWLEDGMENTS

We thank Dr. K. Obata (RIKEN BSI) for providing GAD65 KO mice; Olympus Corp. for technical assistance; and members of the Hensch Lab for discussion, technical assistance, genotyping, and maintenance of mouse colonies. This work was supported by RIKEN BSI and the Japan Science Technology Agency (JST).

Received: March 23, 2006
Revised: January 1, 2007
Accepted: February 27, 2007
Published: March 14, 2007

REFERENCES

Akaaboune, M., Culican, S.M., Turney, S.G., and Lichtman, J.W. (1999). Rapid and reversible effects of activity on acetylcholine receptor density at the neuromuscular junction in vivo. Science *286*, 503–507.

Benevento, L.A., Bakkum, B.W., Port, J.D., and Cohen, R.S. (1992). The effects of dark-rearing on the electrophysiology of the rat visual cortex. Brain Res. *572*, 198–207.

Benevento, L.A., Bakkum, B.W., and Cohen, R.S. (1995). gamma-Aminobutyric acid and somatostatin immunoreactivity in the visual cortex of normal and dark-reared rats. Brain Res. *689*, 172–182.

Bogdanov, Y., Michels, G., Armstrong-Gold, C., Haydon, P.G., Lindstrom, J., Pangalos, M., and Moss, S.J. (2006). Synaptic GABAA receptors are directly recruited from their extrasynaptic counterparts. EMBO J. *25*, 4381–4389.

Chattopadhyaya, B., Di Cristo, G., Higashiyama, H., Knott, G.W., Kuhlman, S.J., Welker, E., and Huang, Z.J. (2004). Experience and activity-dependent maturation of perisomatic GABAergic innervation in primary visual cortex during a postnatal critical period. J. Neurosci. *24*, 9598–9611.

Chattopadhyaya, B., Di Cristo, G., Wu, C.Z., Kuhlman, S.J., Palmiter, R.D., and Huang, Z.J. (2006). GAD67-mediated GABA synthesis and signaling regulate inhibitory synaptic innervation in adolescent visual cortex. CSHL GABA Workshop, p. 7.

Chen, L., Yang, C., and Mower, G.D. (2001). Developmental changes in the expression of GABA(A) receptor subunits (alpha(1), alpha(2), alpha(3)) in the cat visual cortex and the effects of dark rearing. Brain Res. Mol. Brain Res. *88*, 135–143.

Cherubini, E., and Conti, F. (2001). Generating diversity at GABAergic synapses. Trends Neurosci. *24*, 155–162.

Choquet, D., and Triller, A. (2003). The role of receptor diffusion in the organization of the postsynaptic membrane. Nat. Rev. Neurosci. *4*, 251–265.

Christie, S.B., Miralles, C.P., and De Blas, A.L. (2002). GABAergic innervation organizes synaptic and extrasynaptic $GABA_A$ receptor clustering in cultured hippocampal neurons. J. Neurosci. *22*, 684–697.

Dani, V.S., Chang, Q., Maffei, A., Turrigiano, G.G., Jaenisch, R., and Nelson, S.B. (2005). Reduced cortical activity due to a shift in the balance between excitation and inhibition in a mouse model of Rett syndrome. Proc. Natl. Acad. Sci. USA *102*, 12560–12565.

Daw, N. (1995). Visual Development (New York: Plenum).

DeLorey, T.M., Handforth, A., Anagnostaras, S.G., Homanics, G.E., Minassian, B.A., Asatourian, A., Fanselow, M.S., Delgado-Escueta, A., Ellison, G.D., and Olsen, R.W. (1998). Mice lacking the beta3 subunit of the GABAA receptor have the epilepsy phenotype and many of the behavioral characteristics of Angelman syndrome. J. Neurosci. *18*, 8505–8514.

Fagiolini, M., and Hensch, T.K. (2000). Inhibitory threshold for critical-period activation in primary visual cortex. Nature *404*, 183–186.

Fagiolini, M., Pizzorusso, T., Berardi, N., Domenici, L., and Maffei, L. (1994). Functional postnatal development of the rat primary visual cortex and the role of visual experience: dark rearing and monocular deprivation. Vision Res. *34*, 709–720.

Fagiolini, M., Fritschy, J.-M., Löw, K., Möhler, H., Rudolph, U., and Hensch, T.K. (2004). Specific $GABA_A$ circuits for visual cortical plasticity. Science *303*, 1681–1683.

Fritschy, J.-M., and Brünig, I. (2003). Formation and plasticity of GABAergic synapses: physiological mechanisms and pathophysiological implications. Pharmacol. Ther. *98*, 299–323.

Fritschy, J.-M., Paysan, J., Enna, A., and Mohler, H. (1994). Switch in the expression of rat GABAA–receptor subtypes during postnatal development: an immunohisto- chemical study. J. Neurosci. *14*, 5302–5324.

Fritschy, J.-M., Weinmann, O., Wenzel, A., and Benke, D. (1998). Synapse-specific localization of NMDA- and $GABA_A$- receptor subunits revealed by antigen-retrieval immunohistochemistry. J. Comp. Neurol. *390*, 194–210.

Heinen, K., Bosman, L.W.J., Spijker, S., Van Pelet, J., Smit, A.B., Voorn, P., Baker, R.E., and Brussaard, A.B. (2004). $GABA_A$ receptor maturation in relation to eye opening in the rat visual cortex. Neuroscience *124*, 161–171.

Henneberger, C., Kirischyk, S., and Grantyn, R. (2005). Brain-deprived neurotrophic factor modulates GABAergic synaptic transmission by enhancing presynaptic glutamic acid decarboxylase 65 levels, promoting asynchronous release and reducing the number of activated postsynaptic receptors. Neuroscience *135*, 749–763.

Hensch, T.K. (2005). Critical period plasticity in local cortical circuits. Nat. Rev. Neurosci. *6*, 877–888.

Hensch, T.K., and Fagiolini, M. (2005). Excitatory-inhibitory balance and critical period plasticity in developing visual cortex. Prog. Brain Res. *147*, 115–124.

Hensch, T.K., Fagiolini, M., Mataga, N., Stryker, M.P., Baekkeskov, S., and Kash, S.F. (1998). Local GABA circuit control of experience-dependent plasticity in developing visual cortex. Science *282*, 1504–1508.

Hutcheon, B., Fritschy, J.-M., and Poulter, M.O. (2004). Organization of $GABA_A$ receptor α-subunit clustering in the developing rat neocortex and hippocampus. Eur. J. Neurosci. *19*, 2475–2487.

Iwai, Y., Fagiolini, M., Obata, K., and Hensch, T.K. (2003). Rapid critical period induction by tonic inhibition in visual cortex. J. Neurosci. *23*, 6695–6702.

Katz, L.C., and Dalva, M.B. (1994). Scanning laser photostimulation; a new approach for analyzing brain circuits. J. Neurosci. Methods *54*, 205–218.

Kilman, V., van Rossum, M.C.W., and Turrigiano, G.G. (2002). Activity deprivation reduces miniature IPSC amplitude by decreasing the number of postsynaptic $GABA_A$ receptors clustered at neocortical synapses. J. Neurosci. *22*, 1328–1337.

Kittler, J.T., and Moss, S.J. (2003). Modulation of $GABA_A$ receptor activity by phosphorylation and receptor trafficking: implications for the efficacy of synaptic inhibition. Curr. Opin. Neurobiol. *13*, 341–347.

Klausberger, T., Roberts, J.D., and Somogyi, P. (2002). Cell type- and input-specific differences in the number and subtypes of synaptic GABA(A) receptors in the hippocampus. J. Neurosci. *22*, 2513–2521.

Komatsu, Y., and Iwakiri, M. (1991). Postnatal development of neuronal connections in cat visual cortex studied by intracellular recording in slice preparation. Brain Res. *540*, 14–24.

Kunig, G., Leenders, K.L., Sanchez-Pernaute, R., Antonini, A., Vontobel, P., Verhagen, A., and Gunther, I. (2000). Benzodiazepine receptor binding in Huntington's disease: [11C]flumazenil uptake measured using positron emission tomography. Ann. Neurol. *47*, 644–648.

Lewis, D.A., Hashimoto, T., and Volk, D.W. (2005). Cortical inhibitory neurons and schizophrenia. Nat. Rev. Neurosci. *6*, 312–324.

Maffei, A., Nataraj, K., Nelson, A.B., and Turrigiano, G.G. (2006). Potentiation of cortical inhibition by visual deprivation. Nature *443*, 81–84.

Markram, H., Toledo-Rodriguez, M., Wang, Y., Gupta, A., Silberberg, G., and Wu, C. (2004). Interneurons of the neocortical inhibitory system. Nat. Rev. Neurosci. *5*, 793–807.

Morales, B., Choi, S.Y., and Kirkwood, A. (2002). Dark rearing alters the development of GABAergic transmission in visual cortex. J. Neurosci. *22*, 8084–8090.

Morrow, A.L., VanDoren, M.J., Penland, S.N., and Matthews, D.B. (2001). The role of GABAergic neuroactive steroids in ethanol action, tolerance and dependence. Brain Res. Brain Res. Rev. *37*, 98–109.

Mower, G.D. (1991). The effect of dark rearing on the time course of the critical period in cat visual cortex. Brain Res. Dev. Brain Res. *58*, 151–158.

Mower, G.D., Rustad, R., and White, W.F. (1988). Quantitative comparisons of gamma-aminobutyric acid neurons and receptors in the visual cortex of normal and dark-reared cats. J. Comp. Neurol. *272*, 293–302.

Nicoll, R.A. (1994). Cajal's rational psychology. Nature *368*, 808–809.

Nusser, Z., Sieghart, W., Benke, D., Fritschy, J.-M., and Somogyi, P. (1996). Differential synaptic localization of two major γ-aminobutyric acid type A receptor α subunits on hippocampal pyramidal neurons. Proc. Natl. Acad. Sci. USA *93*, 11939–11944.

Nusser, Z., Cull-Candy, S., and Farrant, M. (1997). Differences in synaptic $GABA_A$ receptor number underlie variation in GABA mini amplitude. Neuron *19*, 697–709.

Nusser, Z., Hájos, N., Somogyi, P., and Mody, I. (1998). Increased number of synaptic $GABA_A$ receptors underlies potentiation at hippocampal inhibitory synapses. Nature *395*, 172–177.

Nutt, D.J., and Malizia, A.L. (2001). New insights into the role of the GABA(A)- benzodiazepine receptor in psychiatric disorder. Br. J. Psychiatry *179*, 390–396.

Pettit, D.L., and Augustine, G.J. (2000). Distribution of functional glutamate and GABA receptors on hippocampal pyramidal cells and interneurons. J. Neurophysiol. *84*, 28–38.

Pouille, F., and Scanziani, M. (2004). Routing of spike series by dynamic circuits in the hippocampus. Nature *429*, 717–723.

Prusky, G.T., and Douglas, R.M. (2003). Developmental plasticity of mouse visual acuity. Eur. J. Neurosci. *17*, 167–173.

Rubenstein, J.L., and Merzenich, M.M. (2003). Model of autism: increased ratio of excitation/inhibition in key neural systems. Genes Brain Behav. *2*, 255–267.

Sanes, J.R., and Lichtman, J.W. (2001). Induction, assembly, maturation and maintenance of a postsynaptic apparatus. Nat. Rev. Neurosci. *2*, 791–805.

Sanna, E., Busonero, F., Talani, G., Carta, M., Massa, F., Peis, M., Maciocco, E., and Biggio, G. (2002). Comparison of the effects of zaleplon, zolpidem, and toriazolam at various $GABA_A$ receptor subtypes. Eur. J. Pharmacol. *451*, 103–110.

Soghomonian, J.J., and Martin, D.L. (1998). Two isoforms of glutamate decarboxylase: why? Trends Pharmacol. Sci. *19*, 500–505.

Tanaka, K., Freeman, R.D., and Ramoa, A.S. (1987). Dark-reared kittens: GABA sensitivity of cells in the visual cortex. Exp. Brain Res. *65*, 673–675.

Traynelis, S.G., Silver, R.A., and Cull-Candy, S.G. (1993). Estimated conductance of glutamate receptor channels activated during EPSCs at the cerebellar mossy fiber- granule cell synapse. Neuron *11*, 279–289.

Turrigiano, G.G., and Nelson, S.B. (2004). Homeostatic plasticity in the developing nervous system. Nat. Rev. Neurosci. *5*, 97–107.